Proceedings of the Estonian Academy of Sciences,
2024, **73**, 2, 150–158
https://doi.org/10.3176/proc.2024.2.08
Available online at www.eap.ee/proceedings

MATERIALS
SCIENCE,
ENGINEERING

Mitigation of skull formation in high temperature gas extraction system

Lukas Widder[a*], Karl Adam[b], Martin Egger[b] and Markus Varga[a]

[a] AC2T research GmbH, Viktor-Kaplan-Straße 2/C, 2700 Wiener Neustadt, Austria
[b] voestalpine Stahl GmbH, voestalpine-Straße 3, 4020 Linz, Austria

Received 2 October 2023, accepted 10 November 2023, available online 24 April 2024

Abstract. The adverse impact of particle adhesions and agglomerations on gas flow performance is a prominent concern in high volume extraction systems. The formation of severe skull deposits, involving agglomeration and adhesion processes, particularly at elevated operation temperatures, necessitates labor-intensive and costly manual removal. Consequently, investigating conditions that promote increased skull generation and exploring mechanisms for spontaneous removal through crack formation and chipping are of great significance. This study comprehensively documents the operational conditions of an industrial extraction system, accompanied by elemental gas phase composition analyses. Additionally, the chemical compositions of agglomerated adhesion samples were assessed using X-ray diffraction (XRD) and inductively coupled plasma optical emission spectroscopy (ICP-OES), and their inner structure was examined through SEM. Subsequently, mechanisms leading to these build-ups were simulated on laboratory scale by covering original wall surface samples with agglomeration powder screened for a defined particle size. In experiments conducted at various high temperatures ranging from 800 °C to 1200 °C, while varying the $CaCO_3$ content levels in the powders, a layered structure similar to the real system was successfully acquired. Moreover, under certain defined conditions and different atmospheres, crack formation, significantly impacting the chipping behavior of the skull formations from wall surfaces during application, was observed and the compressive strength was examined. Through our laboratory experiments, specific operating conditions within the calcination cycle were revealed, leading to a substantial enhancement of autonomous discharge of large particle–wall agglomerations. Based on these findings, we propose general process optimization steps to improve the overall performance of the extraction system, such as reduction of fine $CaCO_3$ particles and reduction of the gas flow temperature.

Keywords: adhesion, particle agglomeration, skull formation, high temperature, gas extraction system, compressive strength.

INTRODUCTION

In industrial extraction pipe systems, it is observed that particle–wall agglomeration can result in severe clogging due to deposition and agglomeration processes. The impact is particularly pronounced under high throughput and high temperature operating conditions, leading to a substantial increase in cumulative particle–wall agglomeration processes. This, in turn, can result in the formation of large scale skull deposits on the inner wall surfaces. The presence of these undesired adhesions often necessitates significant human effort and results in costly downtimes for ablation and removal procedures.

In this study, the crucial aspects of pipe clogging and fouling processes were examined, focusing on the deposition of individual particles onto wall surfaces and the agglomeration of multiple particles leading to the formation of bulk material [1–3]. A consequential outcome of these processes is the reduction of the inner pipe diameter, which arises from the cumulative effects of deposition and agglomeration. The intensity of these phenomena is further influenced by various factors, including the combinations of flow turbulences, chemical interactions between particles and wall material, and wall surface properties, such as roughness values [4–6]. Notably, an additional significant effect pertains to wall adhesion and the cohesive forces between particles, which are determined by the composition of gas, temperatures, and the relative

* Corresponding author, lukas.widder@ac2t.at

humidity of both the surrounding air and the gas flow [7–10].

In the typical extraction systems utilized in steelmaking processes, metal vapor tends to condense on dust particles, resulting in exothermic self-sintering phenomena involving iron oxides [11,12]. The composition of the steelmaking dust particles primarily comprises iron and zinc oxides [13,14]. These particles are generated through the bursting of CO gas bubbles and the entrainment of evaporated metals [15,16]. To address the particle generation processes, methods involving flushing with nitrogen [17] or mixed blowing using CO_2 and O_2 have been proposed [15,18]. The mechanical properties in agglomerated materials depend highly on the porosity and size of the particles as well as granule velocity and the surrounding humidity [19–22].

The study focused on examining the stability of severe wall deposits and skull formations in a distinct industrial steelmaking extraction system. Particularly, interest was focused on understanding the conditions that could result in spontaneous material removal through crack formation and chipping. To achieve this goal, detailed documentation of field operating conditions during increased build-up phases and analyses of the elemental gas phase composition were conducted. To comprehend the relevant mechanisms, laboratory experiments were performed to investigate the deposited material under conditions resembling the field environment. Various aspects of the particle and wall material interaction were carefully examined, including variations in temperature and the surrounding atmosphere.

EXPERIMENTAL SECTION

Field operating parameters. Operational data from the field were collected through the utilization of installed on-site sensor systems. These sensor systems continuously measured important parameters during the running operations, including gas flow temperatures, flow rates, volume, the rotational velocities of induced draught fans, and the chemical composition of the gas atmosphere, encompassing H_2, CO, CO_2, N_2, and O_2.

Agglomerate characteristics and temperature effects. To gain an overview of the chemical composition responsible for skull formation, inductively coupled plasma optical emission spectroscopy (ICP-OES) measurements were employed using an Agilent Technologies instrument (5800 VDV, Austria). Phase analyses of the powder adhesions were conducted using powder X-ray diffraction (XRD) with a step size of 0.05° (2Θ) on a Malvern Panalytical instrument (X'Pert Pro MPD, Germany). Further insights into the layered structure and chemical composition were obtained through SEM investigations using a Zeiss device (Ultra 55, Germany), along with EDX (X-Max, Oxford Instruments, UK) analysis. Additionally, a DSC (differential scanning calorimetry) instrument (STA 409 PC, Netzsch, Germany) was employed under various atmospheres, such as N_2, CO_2, and ambient air, with a heating rate of 10 K/min to further investigate characteristic phase transitions and heat flows of the agglomerations.

Adhesion experiments. The primary interest of the experiments was centered on the understanding of agglomeration processes of fine particle dust. To achieve this, original skull formations were collected from various positions with differing temperature levels inside the pipe system. Powder from a specific onsite position where the gas flow temperature was approximately 1000 °C was employed as the standard reference material. It was prepared by grinding and screening to obtain sub-millimeter size (<800 µm) and ensure thorough homogenization.

To conduct adhesion experiments, a custom-built high temperature corrosion test stand (HTCT; see Fig. 1a) was utilized [23]. The experimental arrangement comprised a

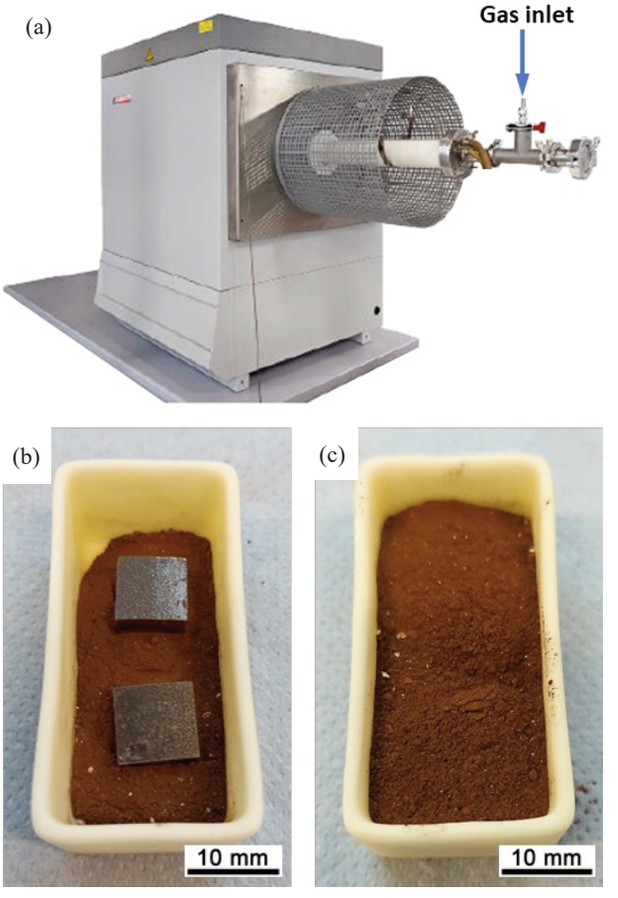

Fig. 1. High temperature corrosion test stand (HTCT) (a), cooling pipe samples embedded in agglomeration powder (b), and covered samples within the crucible (c) (cf. [3]).

tubular furnace equipped with a sparger for insufflation of various gas phases individually or in combination. To mitigate the presence of corrosive oxygen in the atmosphere throughout the experiments, inert nitrogen was predominantly employed. Additionally, carbon monoxide was introduced to replicate a gas phase closely resembling real field conditions. Before CO experiments, nitrogen was employed as the purging agent to remove atmospheric oxygen. During the experiments, gas flow rates of either 1 L/h (N_2) or 0.2 L/h (CO) were employed. The experimental temperature was gradually raised at a rate of 8 °C/min and maintained at a constant level for 90 minutes at one of the designated temperatures: 800 °C, 1100 °C, or 1200 °C. Subsequent to the experimental phase, a controlled gradual cooling process (approximately 3 K/min) was executed under inert nitrogen atmosphere before the furnace was opened. Each experiment involved the utilization of four metallic specimens, with three repetitions carried out for robustness. The experimental procedure consisted of placing two cooling pipe samples adjacent to each other on a bed of 5 g of finely ground agglomeration powder, as illustrated in Fig. 1b. This assembly was situated inside a ceramic crucible made of alumina with the dimensions of 50 × 25 × 20 mm. Following this, an additional 10 g of the powder (Fig. 1c) was layered atop the samples, ensuring that the powder surface levels remained notably below the height of the walls. Notably, the powder was introduced without applying any external pressure. This loose contact between the metal samples aimed to simulate the contact scenario akin to that of particle flow and cooling pipe surfaces within the extraction system.

Layer structure. Following experiments directed towards studying skull formation and layer build-up at temperatures of 800 °C, 1100 °C, and 1200 °C, the metallic specimens were slightly cleaned by removing loose powder and any non-adhering remnants of powder agglomerations. A direct visual inspection was carried out to assess the remaining layer build-up on the metallic sample surfaces. Recognizing the considerable porosity of the adhering layers, the samples underwent infiltration by a thermoplastic resin within a vacuum environment to facilitate embedding and the subsequent cross-sectional analysis. Elemental composition details of the adhering particle agglomerations were revealed through SEM investigations employing a Jeol JIB-4700F microscope (Electron Optics, Japan), coupled with EDX analysis using a Bruker x-Flash 6/30 system (Bruker AXS, Germany).

Generation of fissures. To evaluate changes in crack formation, additional experiments were conducted by adding an extra 15% of $CaCO_3$ content (<700 µm) to the reference powder. To gain further insights, 10 × 10 mm samples were cut from an original, unused metal cooling pipe as usually applied inside the extraction system. These samples were prepared while preserving the pipe's original rolling surface of roughness S_a 5.7 µm. The cooling pipes were composed of low-alloyed 15Mo3 rolled steel and possessed a wall thickness of 4.3 mm. Upon examining the cross sections of the pipe samples, they exhibited a coarse ferritic/pearlitic microstructure. Crack formation was evaluated visually.

In parallel, a distinct set of experiments was conducted to explore the impact of increased $CaCO_3$ content on crack generation within the skull formations. These experiments were exclusively carried out at a temperature of 1100 °C. Similar to the previous set of experiments, the reference powder and the mixture with elevated Ca content were introduced into crucibles without the presence of cooling pipe metal samples. Throughout the testing phase, N_2 or CO gas flows were employed separately. A comprehensive comparison was carried out following the heating cycles regarding the size and distribution of surface cracks under varying experimental conditions.

Strength and stability. For further investigations targeted at the strength and stability of the powder agglomerates after the heating experiments, the tensile testing machine Autograph AG-10TC (Shimadzu, Japan) was applied for uniaxial mechanical testing with load rates of 0.5 mm/min (see Fig. 2). The size differed slightly since there were

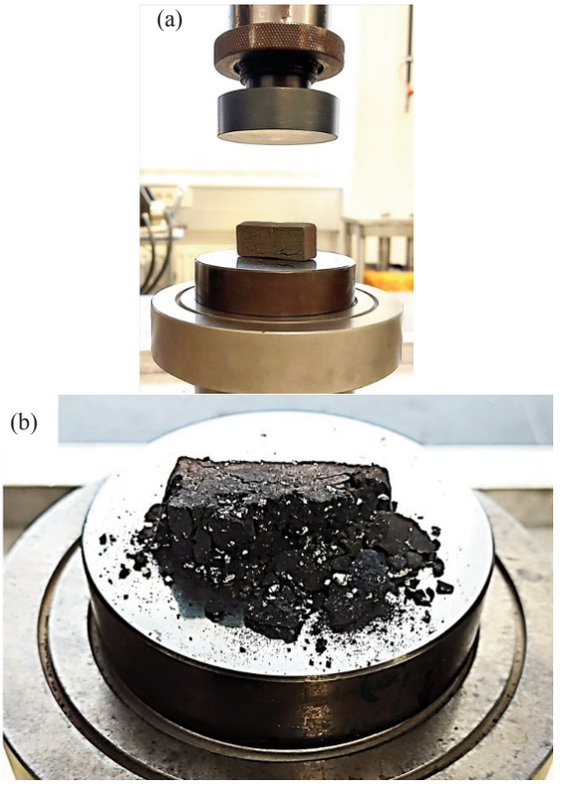

Fig. 2. Setup of a compression test stand including examples of agglomerate samples before (a) and after (b) the compression experiments.

varying sintering shrinkages, but in general the size was roughly 20–25 × 40–45 mm. Apart from the previously used fine $CaCO_3$ particles (<700 µm), an addition of more coarse $CaCO_3$ content (+15 wt%, 1< × <2 mm) was used in sample preparation for compression tests. A minimum of three samples were applied for each set of parameters in the compression experiments.

RESULTS AND DISCUSSION

Field operating parameters

Our examination of agglomeration behavior in a controlled laboratory environment involved detailed record-keeping of the operational conditions encountered during typical field operations. The extraction system is designed to collect dust from a steel pan, resulting in a broad temperature spectrum ranging from approximately 1400 °C to around 250 °C along the complete length of the system. The extraction system inlet exhibited varying flow rates, ranging between 4.3 m/s (during air purging) and 35.8 m/s (during full operation). In totality, the draught fan, operating at approximately 21 s^{-1}, moved around ~22.5 m^3/s. Throughout operational phases, the extracted gas phase demonstrated a composition of roughly 60% CO, 20% CO_2, 15% N_2, and 5% H_2, with an increased proportion of around 80% N_2 observed during recurring purging cycles.

Agglomerate characteristics and temperature effects

By employing ICP-OES analysis, the compositions of various portions of skull formation powder were determined, revealing predominant constituents such as Fe (15–37%), Zn (14–36%), Ca (2–13%), Mn (0.3–3%), and Mg (0.2–2%), as depicted in Fig. 3a. XRD analysis further indicated that these elements were present within the particle–wall agglomerations in diverse forms of oxide structures, as highlighted in Fig. 3b. The elemental ratios exhibited fluctuations depending on the specific location within the extraction system. Notably, regions characterized by higher temperatures displayed reduced zinc content, attributable to its comparatively lower vaporization temperature. Conversely, positions characterized by lower temperatures exhibited elevated zinc content due to higher tendencies for condensation and oxide formation on the wall surface. The contents of the other elements demonstrated a proportional decline towards positions associated with lower temperatures.

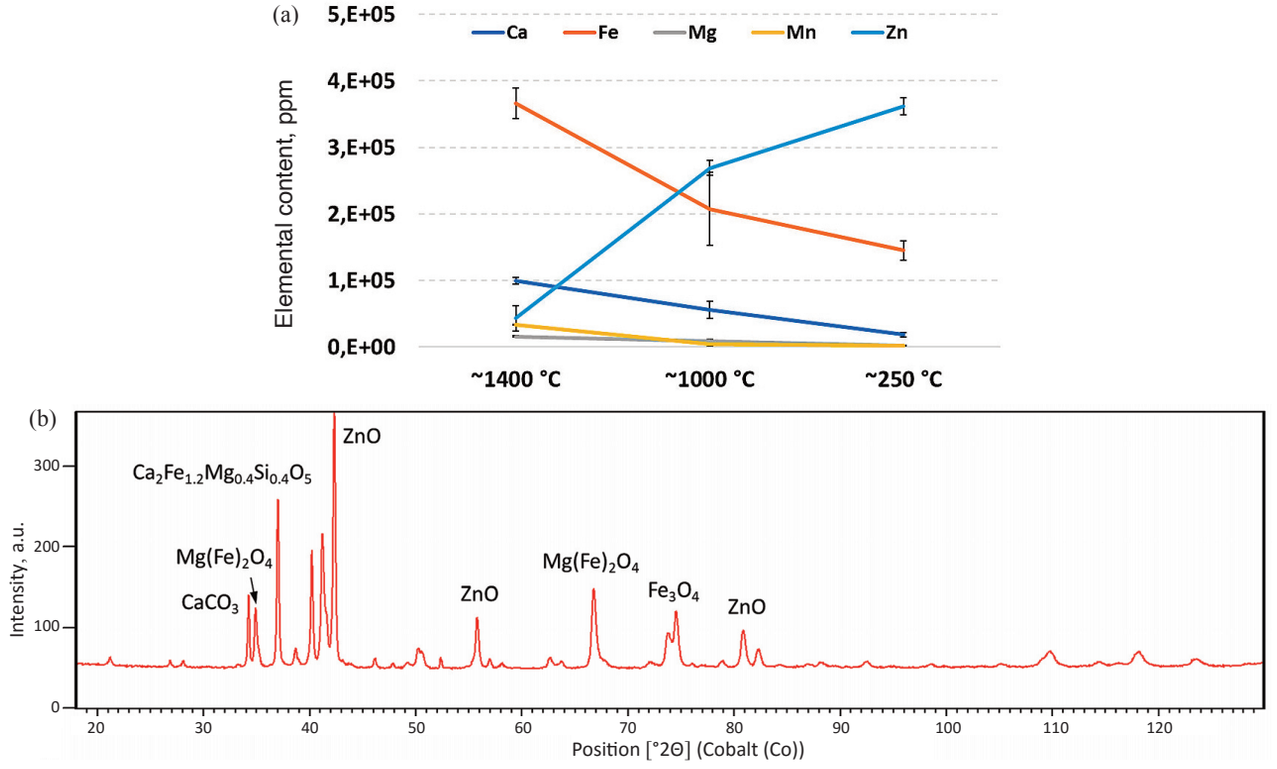

Fig. 3. Chemical composition of different powder samples from original skull formations using ICP-OES (a) and an example of the present oxide content using XRD (b) (cf. [3]).

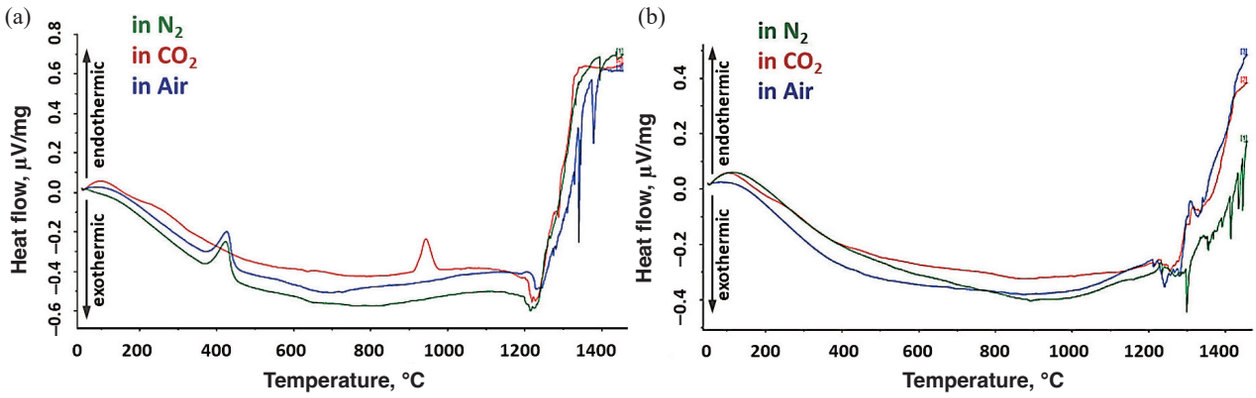

Fig. 4. Distinctive features of reversable oxidation and carbonation processes in DSC analyses of samples after 1100 °C (a), no similar reversible processes evident after testing at 1200 °C (b) (cf. [3]).

To elucidate distinct phase transition mechanisms, supplementary ICP-OES, XRD, and DSC analyses on the resulting agglomerates of the powders were conducted. Following laboratory experiments, ICP-OES revealed comparable trends in powder samples to real field scenarios, wherein higher temperatures correspondingly led to decreased Zn contents. Both XRD and DSC assessments provided further comprehension of the caking processes during the laboratory tests. Notably, DSC analysis under N_2 and CO_2 atmospheres for powder specimens collected post 800 °C and 1100 °C experiments unveiled reversible processes. Specifically, a hydration/dehydration transition of $Mg(OH)_2$ to MgO manifested around 420 °C under N_2, and a carbonization/decarbonization process of $MgCO_3$ to MgO was observed at approximately 780 °C. Under a CO_2 atmosphere, increasing temperatures initiated the carbonization of CaO to $CaCO_3$ until around 920 °C, followed by a reversible conversion to CaO. Beyond roughly 1150 °C, irreversible sintering processes started to occur. Consequently, regardless of the atmospheric conditions, no further occurrence of these reversible processes was noted in the residual powder samples subsequent to the 1200 °C experiments (see Fig. 4).

Consistent with these mechanisms, notable alterations in the visual attributes of the powders were observed. Following the experiments at 800 °C, the powder's initial brown hue remained unchanged and no agglomeration was evident. Elevating the temperature to 1100 °C resulted in a transition to a grey color. While the powder exhibited pronounced agglomeration at this temperature, it retained a notably brittle composition. In contrast, subjecting the powder to the 1200 °C experiments led to its sintering into a robust grey bulk structure.

Layer structure

Further investigations were conducted to examine the progression of the layered arrangement within the initial skull formations, as depicted in Fig. 5a. To this end, a series of three consecutive experiments were carried out, during which samples of the cooling pipes were enveloped with the reference powder. In the subsequent iteration, an extra 15% of $CaCO_3$ content was introduced to the powder. This approach aimed to facilitate the traceability of agglomeration layer development.

Supplementary examinations were conducted to probe the formation of the stratified arrangement within the initial skull formations, displayed in Fig. 5a. Accordingly, in a series of three successive tests, cooling pipe samples were overlaid with reference powder. An extra 15% of $CaCO_3$ content was introduced into the powder during the second iteration. This approach aimed to increase the deducibility of layer structure development.

The SEM/EDX analysis of cross sections yielded variations in the elemental composition of the layers subsequent to experiments conducted at different temperatures. When experiments were conducted at 800 °C and 1100 °C, a comparable pattern in the layer structure emerged. An elemental mapping conducted through EDX analysis unveiled the presence of an initial layer comprising powder agglomerations atop the metal substrate surface of the cooling pipe samples. This initial layer exhibited a thickness of approximately 500 µm, and it showed relatively low concentrations of Ca, consistent with the original composition of the reference powder. As depicted in Fig. 5b, situated above this initial low film was a secondary layer of significantly higher Ca content. This higher Ca content layer corresponded to the additional Ca introduced to the agglomeration powder during the second phase of high-temperature experiments.

In contrast to investigations involving temperatures up to 1100 °C, elevating the temperatures even more induced irreversible sintering processes, leading to distinct variations in the resulting elemental distribution. In the elemental mapping of cross sections following experiments at 1200 °C, the presence of an intermediate layer char-

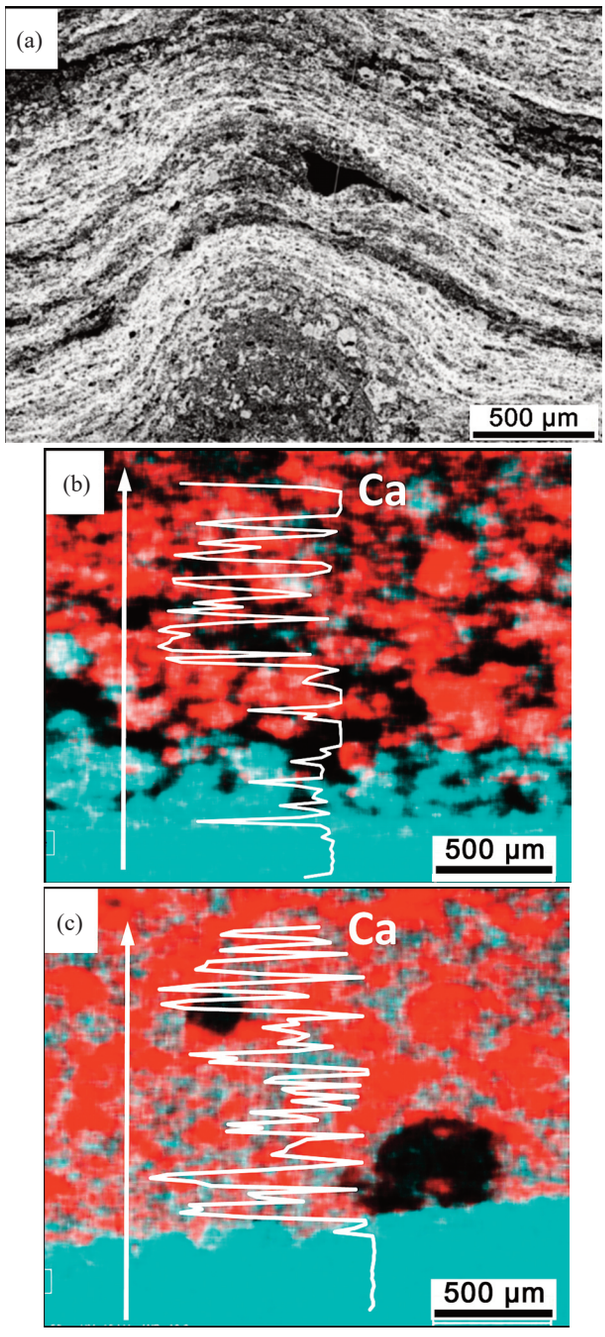

Fig. 5. Layer arrangement within a skull sample in SEM analysis (a), elemental EDX mapping (Ca features in red, Fe features in cyan) and line-scans following HTCT experiments: spatial arrangement after 1100 °C (b) and 1200 °C (c) tests.

acterized by low Ca content was not evident (Fig. 5c). Here, the elevated Ca content exhibited even distribution across all sintered powder conglomerates. Hence, at temperatures roughly above 1200 °C, agglomeration processes experience substantial amplification due to the additive effects of sintering and diffusion, particularly in cases involving higher Ca concentrations. In these scenarios, operational conditions contribute to a more uniform interconnection between two discrete layers of bulk material, while temperatures below 1100 °C result in a more pronounced layer configuration, despite the employment of a comparable experimental setup.

Generation of fissures

To gather supplementary insight into the response under elevated temperatures, a more in-depth examination of the dynamics of spalling and agglomeration was conducted. Therefore, both the reference powder samples and those enriched with an additional 15% of $CaCO_3$ underwent a series of three heating cycles at 1100 °C, with each cycle lasting 90 minutes. Subsequently, we meticulously assessed the configuration of crack and fissure formation on the surface of the resulting sintered ingots. These investigations were thoroughly conducted under two distinct conditions: an inert N_2 environment and a CO atmosphere, which were more representative of the real field conditions.

Initial observations revealed notable sinter shrinkage across all samples contained within the crucibles, alongside a discernible increase in the quantity of white $CaCO_3$ particles. Moreover, Fig. 6 elucidates that specimens featuring augmented Ca content tend to form more densely compacted agglomerations, exhibiting a reduced amount of resulting crack formations. When considering both N_2 and CO atmospheres, the surface of the sintered ingots demonstrated a stronger presence of cracks and fissures in instances where the powder samples contained lower Ca proportions. When applied to real field scenarios, this implies a heightened propensity for spalling and the removal of particle–wall agglomerations through inherent crack formation processes. This tendency is further accentuated when comparing it to densely packed and highly condensed agglomerates that are accompanied by elevated Ca contents within the extracted dust particle flow.

Strength and stability

To assess the strength, additional agglomerate blocks were produced using the HTCT instrument and, subsequently, compression tests were performed. Source materials for the samples included the reference powder as well as reference material containing increased amounts of both fine and coarse $CaCO_3$ particles. The results of the compression experiments indicated significant differences in the load peaks reached as well as in the initial slopes of the curves, which also are directly correlated with the Young's modulus of the sample material. Increasing the

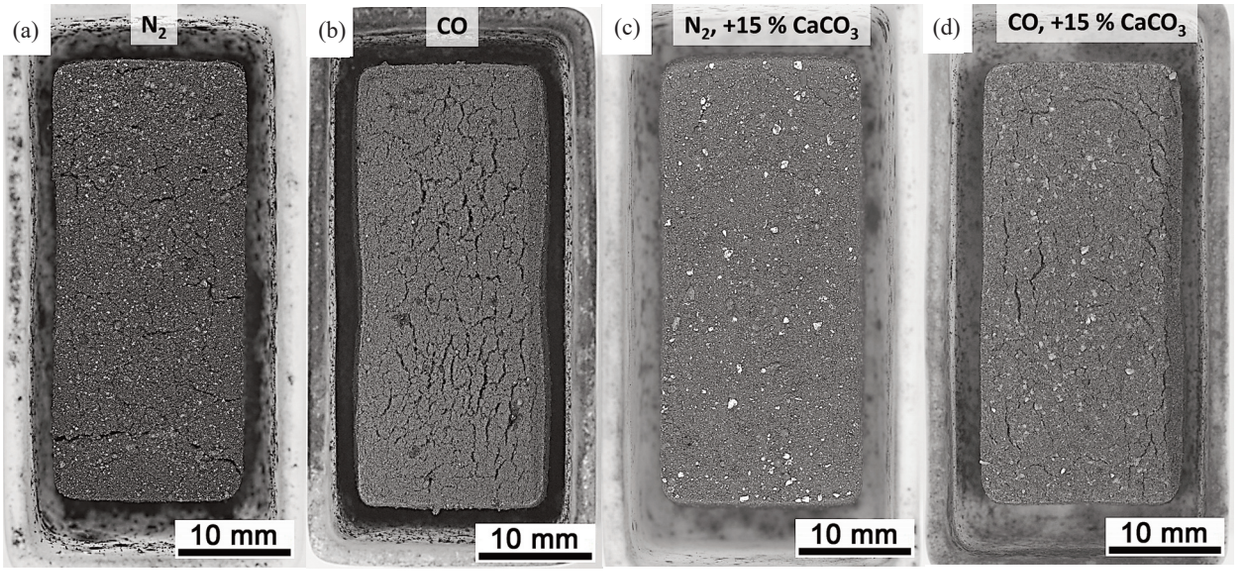

Fig. 6. Fissures and cracks on surfaces of powder agglomerates after HTCT tests at 1100 °C: reference powder in N_2 (a) and CO (b) atmospheres, including added 15% of $CaCO_3$ content in N_2 (c) and CO (d) atmospheres (cf. [3]).

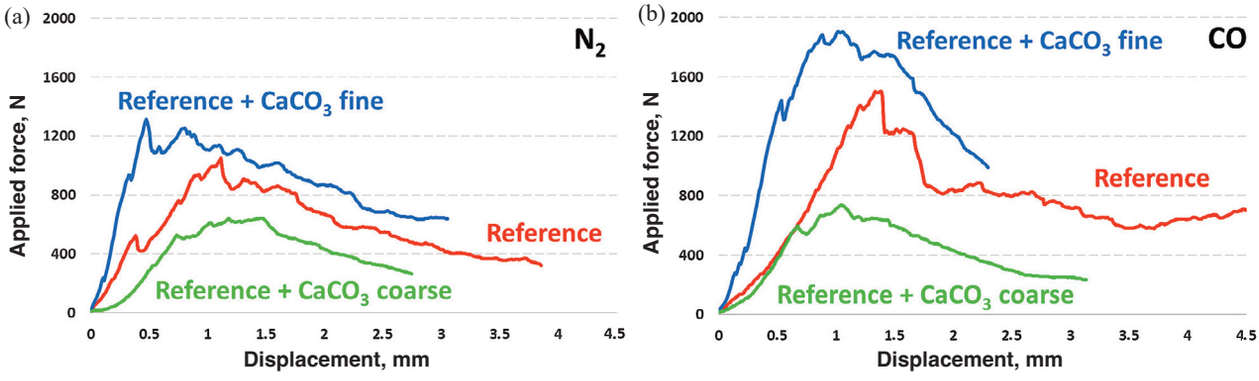

Fig. 7. Average curves of compression test results from reference powder agglomerates, including additional amounts of fine and coarse $CaCO_3$ generated in N_2 (a) and CO (b) atmospheres.

fine $CaCO_3$ content resulted in significantly higher strength values for specimens produced in N_2 and in CO, and in higher resistances to deformation (higher Young's modulus). Conversely, when coarse $CaCO_3$ particles were added, the blocks withstood only significantly lower loads and exhibited reduced stability. Compared with specimens prepared in N_2, the specimens generated in CO displayed a distinct tendency toward significantly enhanced strength. The two diagrams for experiments in N_2 and CO atmospheres are displayed in Fig. 7 and show an average of at least three data points for each position.

CONCLUSIONS

The central focus of this investigation revolved around particle–wall agglomerations within a high temperature, high volume extraction system. Excessive adhesions not only disrupt the extraction flow but also demand substantial maintenance interventions due to the unwelcome formation of skull deposits. Consequently, both the chemical composition and the factors contributing to amplified agglomeration were subjected to comprehensive examination. Owing to the relatively modest vaporization temperatures of Zn, its concentration increased in regions characterized by lower temperatures, thereby resulting in

higher levels of Fe, Ca, and Mg in areas experiencing higher temperatures, roughly around 1100 °C. Notably, reversible reaction processes predominantly involve Mg- and Ca-oxides at these elevated temperatures. As the temperatures at certain positions within the extraction system exceed the 1200 °C threshold, irreversible sintering processes become prominent, triggering the creation of dense skull deposits. Laboratory experiments underscored the potential for altering the layered build-up, though at 1200 °C, the distinctive layered structure became imperceptible. Furthermore, reduced amounts of $CaCO_3$ exerted a substantial influence on crack formations, thereby affecting the potential for spalling initiation and reducing the expansion of particle–wall agglomerations. Moreover, compression experiments revealed significantly higher agglomerate stability and Young's modulus in the presence of increased amounts of fine $CaCO_3$ particles. The prospective system optimization approach aims to reduce fine $CaCO_3$ particle absorption by (i) strategically using screening mechanisms, specific mesh sizes, and compaction systems and (ii) minimizing immediate extraction during processing. Additionally, it involves controlling gas extraction system temperatures below 1200 °C to prevent crack formation, maintain reversible reactions, and reduce sintering.

ACKNOWLEDGMENTS

This work was funded by the Austrian COMET-Program (project InTribology1, No. 872176) via the Austrian Research Promotion Agency (FFG) and the federal states of Niederösterreich and Vorarlberg and was carried out within the Excellence Centre of Tribology (AC2T research GmbH). The publication costs of this article were partially covered by the Estonian Academy of Sciences.

REFERENCES

1. Henry, C. Surface forces and their application to particle deposition and resuspension. In *Particles in Wall-bounded Turbulent Flows: Deposition, Re-suspension and Agglomeration* (Minier, J.-P. and Pozorski, J., eds). Springer, Cham, 2017, 209–261. https://doi.org/10.1007/978-3-319-41567-3_5
2. Minier, J.-P. A general introduction to particle deposition. In *Particles in Wall-bounded Turbulent Flows: Deposition, Re-suspension and Agglomeration* (Minier, J. P. and Pozorski, J., eds). Springer, Cham, 2017, 1–36. https://doi.org/10.1007/978-3-319-41567-3
3. Widder, L., Adam, K., Egger, M. and Varga, M. Mechanisms and prevention of skull formation in high temperature gas extraction system. *AIP Conf. Proc.*, 2024, **2898**(1), 030001. https://doi.org/10.1063/5.0189466
4. Henry, C. and Minier, J.-P. Progress in particle resuspension from rough surfaces by turbulent flows. *Prog. Energy Combust. Sci.*, 2014, **45**, 1–53.
5. Wang, X., You, C., Liu, R. and Yang, R. Particle deposition on the wall driven by turbulence, thermophoresis and particle agglomeration in channel flow. *Proc. Combust. Inst.*, 2011, **33**(2), 2821–2828. https://doi.org/10.1016/j.proci.2010.08.009
6. Khalifa, A. and Breuer, M. An efficient model for the breakage of agglomerates by wall impact applied to Euler–Lagrange LES predictions. *Int. J. Multiph. Flow.*, 2021, **142**, 103625. https://doi.org/10.1016/j.ijmultiphaseflow.2021.103625
7. Giffin, A. and Mehrani, P. Effect of gas relative humidity on reactor wall fouling generated due to bed electrification in gas-solid fluidized beds. *Powder Technol.*, 2013, **235**, 368–375. https://doi.org/10.1016/j.powtec.2012.10.037
8. Jones, R., Pollock, H. M., Geldart, D. and Verlinden, A. Inter-particle forces in cohesive powders studied by AFM: effects of relative humidity, particle size and wall adhesion. *Powder Technol.*, 2003, **132**(2–3), 196–210. https://doi.org/10.1016/S0032-5910(03)00072-X
9. Shotton, E. and Harb, N. The effect of humidity and temperature on the cohesion of powders. *J. Pharm. Pharmacol.*, 1966, **18**(3), 175–178. https://doi.org/10.1111/j.2042-7158.1966.tb07844.x
10. Varga, M., Rojacz, H., Widder, L. and Antonov, M. High temperature erosion-corrosion of wear protection materials. *J. Bio- Tribo-Corros.*, 2021, **7**(3), 87. https://doi.org/10.1007/s40735-021-00504-9
11. Longbottom, R. J., Monaghan, B. J., Pinson, D. J. and Chew, S. J. Understanding the self-sintering process of BOS filter cake for improving its recyclability. *J. Sustain. Metall.*, 2019, **5**, 429–441. https://doi.org/10.1007/s40831-019-00233-x
12. Peng, B., Chai, L.-Y., Song, H.-C., Peng, J., Min, X.-B., Wang, Y.-Y. et al. Study on stainless steelmaking dust agglomeration. *J. Cent. South Univ. Technol.*, 2004, **11**, 45–50. https://doi.org/10.1007/s11771-004-0010-9
13. Krztoń, H. J. 2010. Quantitative phase composition of steelmaking dust from polish steel industry. *Solid State Phenom.*, 2010, **163**, 31–37.
14. Vereš, J., Šepelák, V. and Hredzák, S. Chemical, mineralogical and morphological characterisation of basic oxygen furnace dust. *Miner. Process. Extr. Metall.*, 2015, **124**(1), 1–8. https://doi.org/10.1179/1743285514Y.0000000069
15. Li, Z., Zhu, R., Ma, G. and Wang, X. Laboratory investigation into reduction the production of dust in basic oxygen steelmaking. *Ironmak. Steelmak.*, 2017, **44**(8), 601–608. https://doi.org/10.1080/03019233.2016.1223906
16. Delhaes, C., Hauck, A. and Neuschütz, D. Mechanisms of dust generation in a stainless steelmaking converter. *Steel Res.*, 1993, **64**, 22–27.
17. Steer, J., Grainger, C., Griffiths, A., Griffiths, M., Heinrich, T. and Hopkins, A. Characterisation of BOS steelmaking dust and techniques for reducing zinc contamination. *Ironmak. Steelmak.*, 2014, **41**(1), 61–66.
18. Yi, C., Zhu, R., Chen, B.-Y., Wang, C.-R. and Ke, J.-X. Experimental research on reducing the dust of BOF in CO2 and O2 mixed blowing steelmaking process. *ISIJ Int.*, 2009, **49**(11), 1694–1699. https://doi.org/10.2355/isijinternational.49.1694

19. Russell, A., Schmelzer, J., Müller, P., Krüger, M. and Tomas, J. Mechanical properties and failure probability of compact agglomerates. *Powder Technol.*, 2015, **286**, 546–556.
20. Van der Zwan, J. and Siskens, C. A. M. The compaction and mechanical properties of agglomerated materials. *Powder Technol*., 1982, **33**(1), 43–54.
21. Meissner, H. P., Michaels, A. S. and Kaiser, R. Crushing strength of zinc oxide agglomerates. *Ind. Eng. Chem. Process Des. Dev.*, 1964, **3**(3), 202–205.
22. Bika, D. G., Gentzler, M. and Michaels, J. N. Mechanical properties of agglomerates. *Powder Technol.*, 2001, **117**(1–2), 98–112.
23. Priss, J., Klevtsov, I. and Winkelmann, H. High-temperature chlorine corrosion in presence of sulfur containing and potassium external deposits. In *Proceedings of the 23rd International DAAAM Symposium, Zadar, Croatia, 21–28 October 2012*. DAAAM International, Vienna, Austria, 2012, 0911–0916.

Ripptäidise tekke vähendamine kõrgtemperatuursetes gaasiärastussüsteemides

Lukas Widder, Karl Adam, Martin Egger ja Markus Varga

Osakeste kokkukleepumise ja kuhjumise negatiivne mõju gaasivoolule tekitab kõrgtootlikes ärastussüsteemides suuri probleeme. Paksude ripptäidisest settekihtide kuhjumine ja kokkukleepumine, eriti kõrgetel temperatuuridel, tingib töömahuka ja kuluka käsitsi eemaldamise vajaduse. Seetõttu on oluline uurida tingimusi, mis soodustavad intensiivset ripptäidise teket, ning mehhanisme selle spontaanseks lagunemiseks pragunemise ja kildumise teel.

Uurimus annab põhjaliku ülevaate tööstusliku ärastussüsteemi käitustingimustest. Uurimistöö käigus analüüsiti gaasifaasi koostist. Lisaks uuriti röntgendifraktomeetria ja induktiivsidestatud plasma optilise emissiooni spektromeetria abil ripptäidise proovide keemilist koostist ja vaadeldi skaneeriva elektronmikroskoobiga nende sisestruktuuri. Seejärel taasloodi setete tekkemehhanismid laboratoorsetes tingimustes, kattes esialgsest seinamaterjalist välja lõigatud proovikehad setetest sõelutud kindla suurusega pulbriga. Erinevatel kõrgetel temperatuuridel (800–1200 °C) läbi viidud katsetes, mille käigus varieeriti $CaCo_3$ sisaldust pulbrites, saadi reaalses ärastussüsteemis tekkivaga sarnane kihiline struktuur. Teatud kindlaksmääratud tingimustes ja erinevates keskkondades täheldati pragunemist, mis mõjutas tugevalt ripptäidise mahakoorumist torude sisepinnalt kasutamise käigus, ning uuriti survetugevust. Laboratoorsete katsete käigus määratleti konkreetsed kaltsineerimistsükli käitustingimused, mis märgatavalt võimendavad suurte settekihtide isekoorumist. Uurimuse tulemuste põhjal pakutakse välja üldised optimeerimisvõimalused ärastussüsteemi tõhususe parandamiseks, näiteks $CaCO_3$ peente osakeste osakaalu ja gaasivoolu temperatuuri vähendamine.